THE ASTROPHYSICAL JOURNAL, 402:L37–L40, 1993 January 10

DISCOVERY OF AN OPTICAL SYNCHROTRON JET IN 3C 264[1]

P. CRANE,[2,3] R. PELETIER,[3] D. BAXTER,[4] W. B. SPARKS,[4] R. ALBRECHT,[2,5,6] C. BARBIERI,[2,7] J. C. BLADES,[2,4]
A. BOKSENBERG,[2,8] J. M. DEHARVENG,[2,9] M. J. DISNEY,[2,10] P. JAKOBSEN,[2,6] T. M. KAMPERMAN,[2,11]
I. R. KING,[2,12] F. MACCHETTO,[2,4,6] C. D. MACKAY,[2,13] F. PARESCE[2,4,6,14]
G. WEIGELT,[2,15] P. GREENFIELD,[4] R. JEDRZEJEWSKI,[4] AND A. NOTA[4,7]
Received 1992 July 26; accepted 1992 October 28

ABSTRACT

Observations with the Faint Object Camera on board the *Hubble Space Telescope* have revealed a new optical jet in the core of the elliptical galaxy NGC 3862 (3C 264). Morphologically, this jet is similar to the synchrotron jets seen in other galaxies, as it shows knots and bifurcations. The optical spectral index $[-d \log I(\nu)/d \log \nu = \alpha = 1.4]$ is also similar to that found in other jets. Thus, the nucleus of NGC 3862 appears to contain the fifth known example of an optical synchrotron jet. Since NGC 3862 is a typical radio-loud elliptical galaxy, it seems likely that many nonthermal jets found in the radio continuum may also have optical counterparts.

Subject headings: galaxies: individual (NGC 3862) — galaxies: jets — radiation mechanisms: miscellaneous

1. INTRODUCTION

NGC 3862 (3C 264) is optically the sixth-brightest galaxy in the cluster Abell 1367. Its radial velocity of 6462 km s^{-1} puts it at a distance of 86.2 Mpc for $H_0 = 75$ km s^{-1} Mpc^{-1}. The radio luminosity and morphology classify it as Fanaroff-Riley Type 1 (Fanaroff & Riley 1974). It contains an unresolved and possibly variable X-ray source (Elvis et al. 1981). This galaxy was observed in two bands with the Faint Object Camera in the course of a program to study the nuclei of nearby galaxies (Crane et al. 1992). Surprisingly, both the images obtained showed a prominent jetlike feature emanating from the nucleus (see Fig. 1 [Pl. L2]) and reminiscent of the jet in M87 (Boksenberg et al. 1992). This *Letter* reports some details of this unexpected discovery.

3C 264 is a head-tail radio source (Gavazzi, Perola, & Jaffe 1981) and has been included in the studies of radio galaxies by Baum, Heckman, & van Breugel (1992 and references therein). The existence of a jetlike feature in the VLA maps at roughly the same position angle as that found by the *Hubble Space Telescope* was noted by Gavazzi et al. (1981). The apparent low-ionization state of the nuclear region was reported by Baum et al. (1992). Unfortunately, the angular resolution of the VLA and the ground-based optical data is not good enough to make definitive statements about the jet described here.

Jets and jetlike structures are seen in many powerful radio galaxies. However, the optical counterparts to synchrotron jets have been seen previously in only four sources: M87, 3C 273, 3C 66B, and PKS 0521−36 (Meisenheimer et al. 1989; Macchetto et al. 1991a, b; Biretta, Stern, & Harris 1991). Optical synchrotron jets, as opposed to hot spots (3C 33) and knots (Coma A), show elongated structure with an obvious connection to the nucleus. Thus the discovery of an optically visible jet, which may be the fifth synchrotron jet, is of interest.

Jets are the result of energy transported out of the nucleus of the parent galaxy in a collimated beam. The mechanism for the collimation is not well understood but is thought to be due either to the magnetic field structure in and around the galaxy or to an intrinsic anisotropy in the radiation source itself. The anisotropy could be along a rotation axis or could be associated with an accretion disk. In the standard scenarios, the radio and optical emission from jets arises from the interaction of the jet with the surrounding medium. If the jet consists of relativistic particles, then they will produce synchrotron radiation as their trajectories are bent by the magnetic field lines. If the jet consists of radiation, then the radiation will heat the surrounding medium, which again emits synchrotron radiation in the magnetic field. The previously known jets are well explained by scenarios of this kind, since the synchrotron nature of the emission is well established from observations of the spectra and polarizations.

2. OBSERVATIONS AND ANALYSIS

NGC 3862 was observed with the Faint Object Camera (FOC) on board the *Hubble Space Telescope* (*HST*) on 1992 January 22 using the f/96 optical chain. One exposure of 905 s was obtained with the F342W filter which is centered at 3400 Å and roughly 700 Å wide (see Paresce 1992 for details of the FOC filters). A second exposure of 596 s was obtained with the F502M filter, which is centered at 4850 Å with a width of roughly 400 Å. The filters do not approximate any ground-based filter system very well, but will be referred to as the *U*

[1] Based on observations with the NASA/ESA *Hubble Space Telescope*, obtained at the Space Telescope Science Institute, which is operated by the Association of Universities for Research in Astronomy, Inc., under NASA contract NAS 5-26555.

[2] Member, Faint Object Camera Investigation Definition Team.
[3] European Southern Observatory, D-8046 Garching, Germany.
[4] Space Telescope Science Institute, Baltimore, MD 21218.
[5] Space Telescope European Coordinating Facility, D-8046 Garching, Germany.
[6] Astrophysics Division, Space Science Department of the European Space Agency, F-75738 Paris Cedex 15, France.
[7] Osservatorio Astronomico di Padova, I-35122, Padova, Italy.
[8] Royal Greenwich Observatory, Cambridge, CB3 0EZ, England.
[9] Laboratoire d'Astronomie Spatiale du Centre National de la Recherche Scientifique, F-13012 Marseilles, France.
[10] Department of Physics, University College of Cardiff, Cardiff CF4 3TH, Wales.
[11] Laboratory for Space Research Utrecht, 3584 CA, Utrecht, The Netherlands.
[12] Astronomy Department, University of California, Berkeley, Berkeley, CA 94720.
[13] Institute of Astronomy, Cambridge, CB3 0HA, England.
[14] Osservatorio Astronomico di Torino, Turin, Italy.
[15] Max-Planck-Institut für Radioastronomie, D-5300 Bonn, Germany.

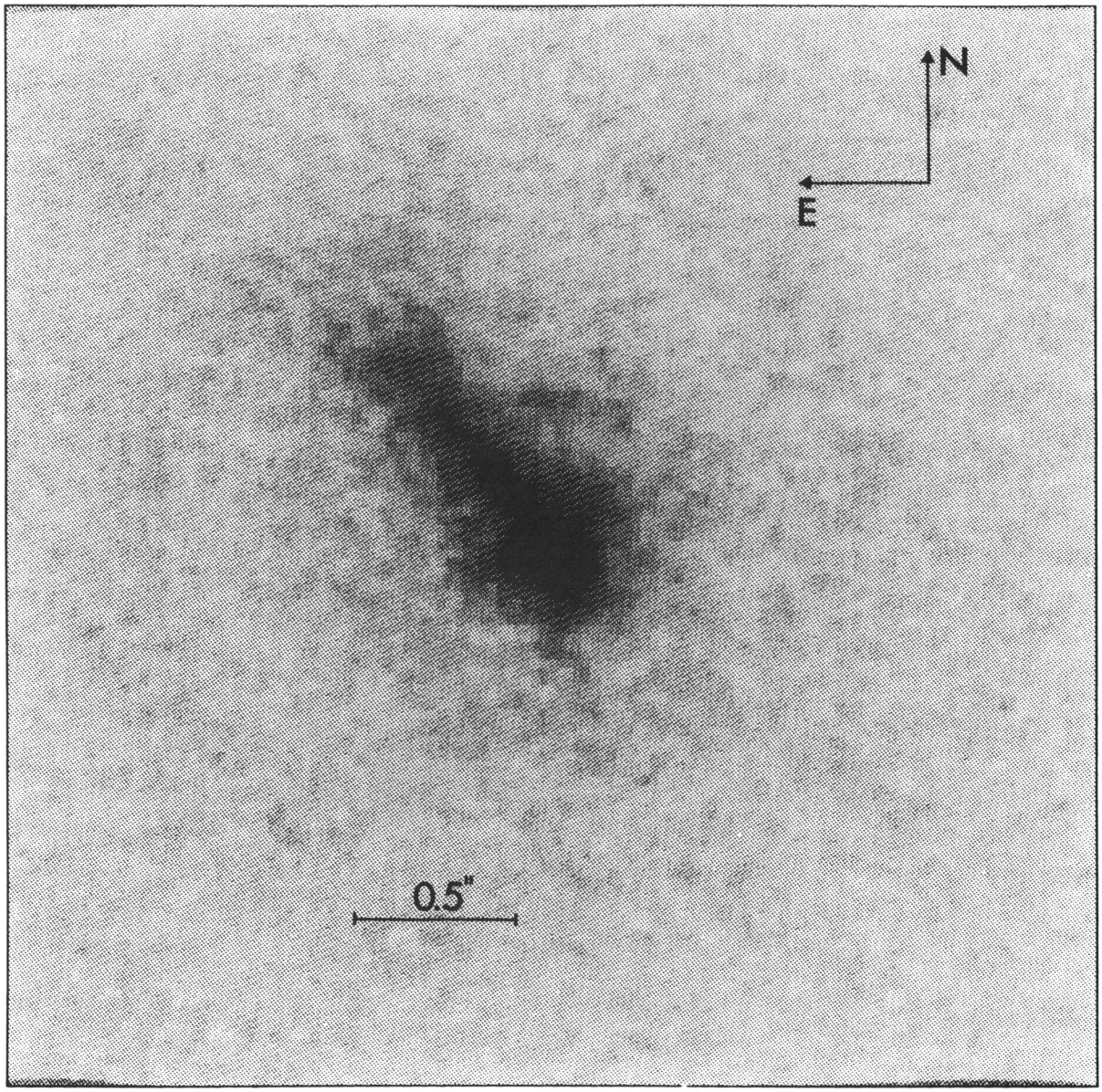

FIG. 1.—FOC image taken at 3400 Å of the central region of the galaxy NGC 3862. The new jetlike feature is clearly seen. Several knots and twists are evident. The image has a resolution of about 0".06, and the total length of the jet is about 0".65. The reseau marks on the FOC photo cathode have been smoothed over, and the image has been rotated to bring the *y*-axis to north.

CRANE et al. (see 402, L37)

and *B* filters in the following, and fluxes will be compared to the ground-based results in the well-defined Johnson filter system. The raw data were processed using the standard procedures to flat-field and geometrically correct the FOC images. The FOC f/96 optical train has a field of view of 11″ × 11″, and the individual pixels subtend 0.″0224. The data were taken with the spacecraft in fine lock, which provides a jitter of roughly 0.″007. Figure 1 shows the F342W image in very close to its original form.

The signal-to-noise ratio of the jet in the F342W filter is considerably better than in the F502M filter because the jet is relatively brighter in *U* and because the net FOC sensitivity is better in the F342W filter. Since the observations were planned to study what was expected to be a weak blue component of the stellar population, roughly similar signal-to-noise ratios were anticipated in each filter for the stellar population normally found in early-type galaxies.

Both images were deconvolved using the standard deconvolution package included in the STSDAS package (Lucy 1974). Figures 2*a* and 2*b* (Plates L3 and L4) show the result of 100 iterations of this algorithm for the F342W and F502M images. All of the features suspected in Figure 1 are clearly seen in both Figure 2*a* and Figure 2*b*. The jet is seen in both *U* and *B* exposures, and, in addition, the details are very similar in all the images. Figure 3 shows a contour plot of the *U* exposure.

The position angle of the jet is 37°, which is very close to the position angle of the radio jet seen at much lower resolution (Gavazzi et al. 1981). The jet is approximately 0.″65 long to the point of bifurcation seen in the figures. At the distance of NGC 3862, this corresponds to a length of 270 pc for the jet. This should be compared with the jet in M87, which is about 2.1 kpc in length (Boksenberg et al. 1992), and the jet in 3C 66B, which is about 3 kpc long (Macchetto et al. 1991b). Thus this jet is shorter than the other known synchrotron jets.

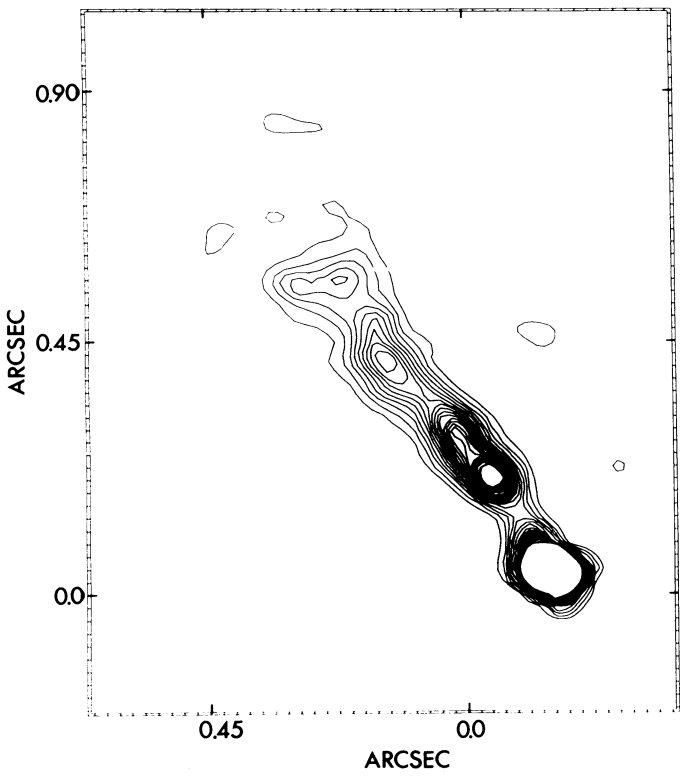

FIG. 3.—Contours of the *U* image seen in Fig. 2*a*. At least five peaks in the emission are seen in the contour map at this wavelength.

2.1. *Flux Calibration*

The relative sensitivity of the two filters has been determined using a simulator of the FOC response function. In-orbit tests of the FOC sensitivity confirm that the sensitivity tables used are accurate to within 5%. Basically, the simulator determines the number of detected photons for a known input spectrum using the response curves for the filters and for FOC detectors. For an input spectral flux of the form $S(\nu) \propto \nu^{-\alpha}$, the ratio of the number of detected photons in the F342W to that in the F502M filters is expected to be 5.08 for $\alpha = 1$. For a spectrum with a power-law index of $\alpha = 1.4$ instead of 1.0, this ratio becomes 4.35. This choice of spectral index is explained below and in Figure 4.

In addition, the standard FOC calibration procedures also provide data necessary to estimate the absolute fluxes. The flux in μJy is given by:

$$\mathcal{F}_\nu = \mathcal{R}\,\frac{\lambda_p^2}{c}\,U \times 10^{29}\ ,$$

where $\mathcal{R}$ is the count rate per second from the source, λ_p is the "pivot" wavelength (Kornneef et al. 1985) in angstroms for the filter used, and *U* is the inverse sensitivity of the FOC in ergs cm^{-2} counts^{-1}. The pivot wavelengths and the inverse sensitivities are found in the image headers. This technique and the previous one yield essentially identical results.

Using the published photometry and colors (Sandage 1973; Véron-Cetty 1984), we have compared the colors derived from the *U* and *B* *HST* images with the $U-B$ colors of the stellar continuum outside the region of the nucleus and the jet. A very rough conversion from $(U-B)_{\rm FOC}$ to Johnson $(U-B)_{\rm J}$ was derived by Crane et al. (1993), using the STSDAS routine SYNPHOT and a library of various stars. This relation is $(U-B)_{\rm FOC} = 1.8(U-B)_{\rm J} + 0.4$. For the outer regions of the galaxy we find $(U-B)_{\rm FOC} = 1.5 \pm 0.1$, which would predict

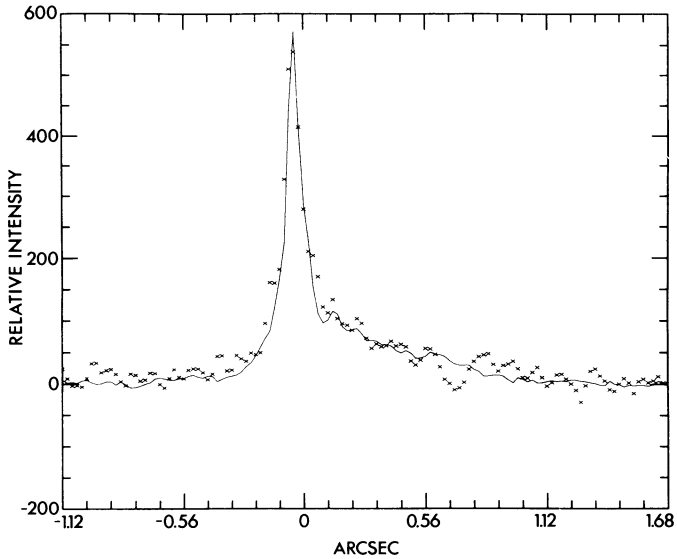

FIG. 4.—Plot of the flux along the jet in the *U* band (*solid line*; individual points are connected) and in the *V* band (*crosses*). Note the detailed match between the flux in these two bands. The *U*-band data have been divided by 6.6, which is 4.35 times the ratio of exposure times.

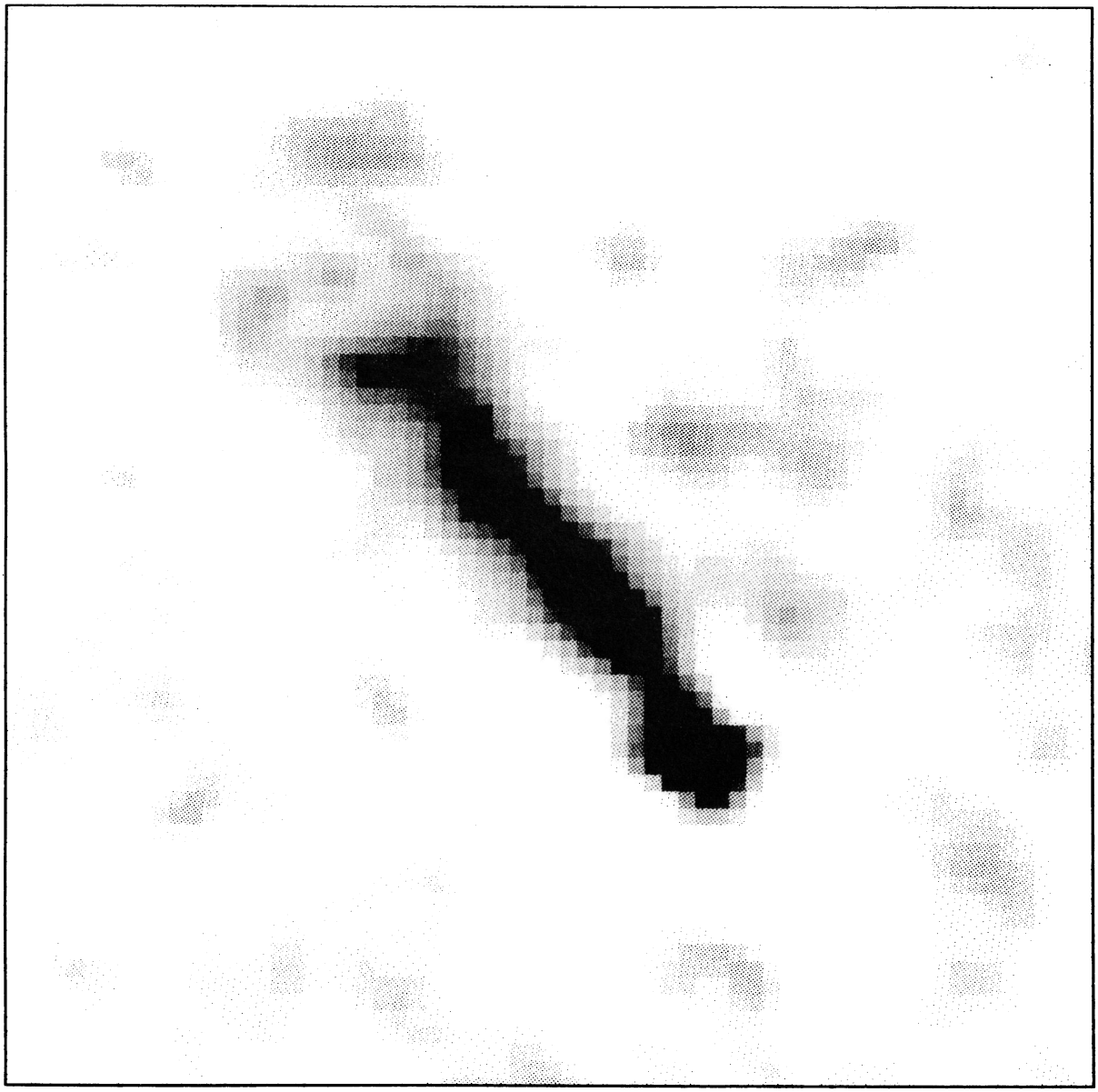

FIG. 2*a*

FIG. 2.—(*a*) This image shows the results of deconvolving Fig. 1 using 100 iterations of the Lucy algorithm. The twists and knots are now clearly visible. (*b*) Result of 100 iterations of the Lucy algorithm on the *V* image. The bifurcation at the end of the jet is more evident here, although the signal-to-noise ratio is lower than for the *U* image.

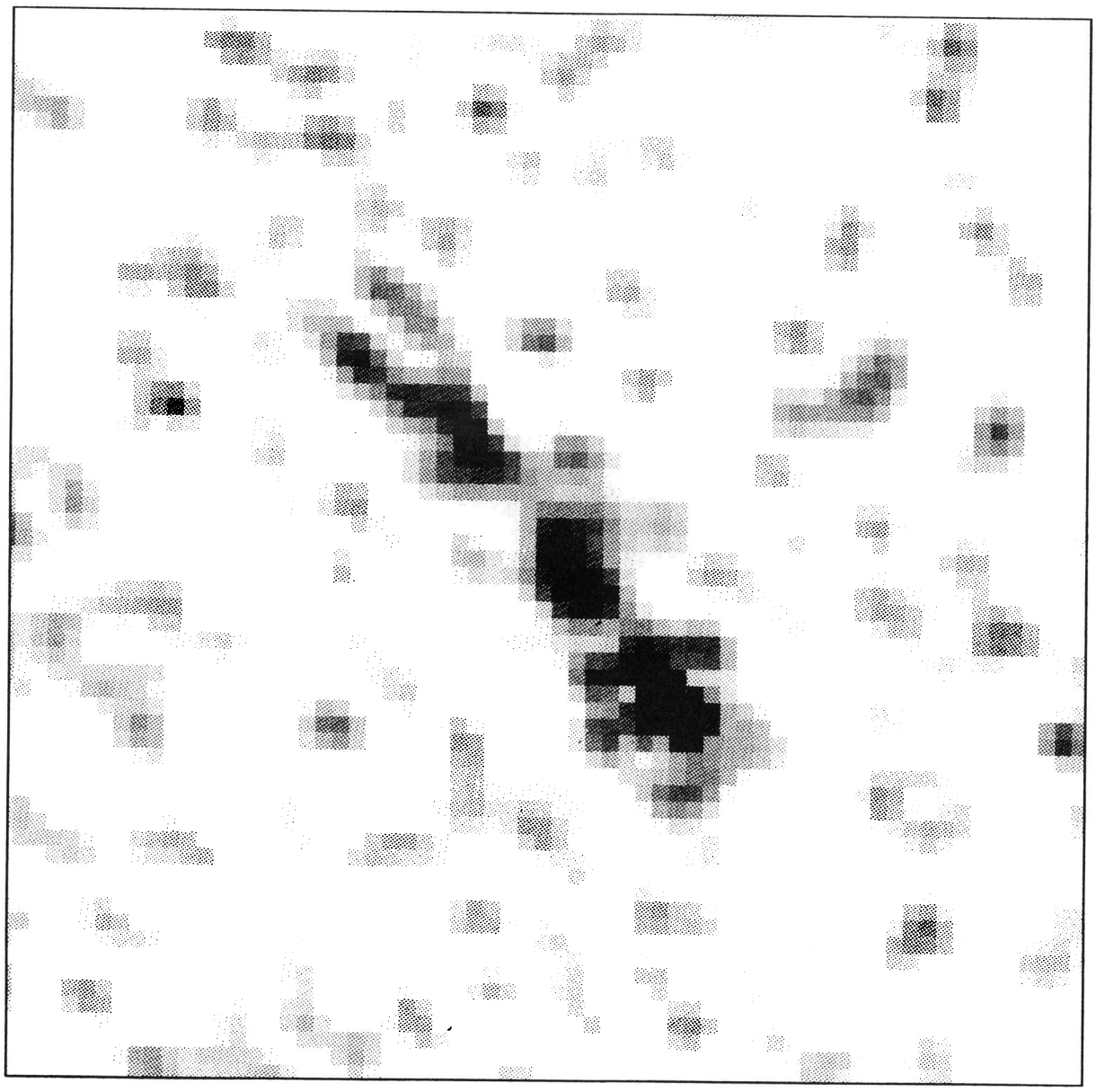

FIG. 2*b*

CRANE et al. (see 402, L38)

$(U-B)_J \approx 0.61$. This can be compared with the ground-based value of $U-B=0.49$. Considering that the filters do not match well and color terms are certainly expected, this correspondence is considered satisfactory.

2.2. *Spectral Index*

In order to estimate the spectral index of the jet and the nucleus, the pixels perpendicular to the jet in the undeconvolved image were summed in a section 20 pixels wide centered on the jet. An adjacent section, also 20 pixels wide, was used as the background and was subtracted from the first to yield the flux in the jet and nucleus alone. Of course this procedure is not perfect, since the galaxy contribution is slightly different in the two sections. However, since the jet is considerably brighter than the galaxy and the galaxy profile outside the nucleus is fairly flat, this small difference is unimportant. We note that if we measure the flux and spectral index using the deconvolved images, the errors are even more complicated to evaluate.

The flux calibration numbers given above for $\alpha = 1.4$, and the ratio of exposure times, were then used to divide the *U* image by 6.60. The extracted profiles for both the *U* and the *B* images are shown in Figure 4. The very good match between the two profiles implies that the spectral index of the jet is very close to 1.4. This result assumes that the emission seen in the images is entirely continuum emission and not line emission. We have obtained a spectrum of the nucleus of NGC 3862 with the ESO NTT in the range from 3700 to 6000 Å. We find no evidence for emission features, although the signal-to-noise ratio is rather poor. Nevertheless, we can safely state that contamination by emission features is not seriously distorting the determination of the spectral index. No correction for Galactic interstellar extinction has been made.

In order to check the above procedure, a similar exercise was carried out on the deconvolved images of Figure 2. This gave a spectral index of 1.2 for the jet and 1.4 for the nucleus. These can be compared with the values determined above, and the differences should be considered as indicative of the uncertainties in the data and procedures.

Thus the spectral indices are similar to those found for M87 and 3C 273 (Meisenheimer 1991). The spectral index and several other properties of 3C 264 are compared in Table 1. The nuclear spectral index is relatively close to the nuclear spectral index of 1.37 found for M87 by Boksenberg et al. (1992). Therefore, based on the spectral indices, the jet seems quite similar to the other synchrotron jets that have been studied.

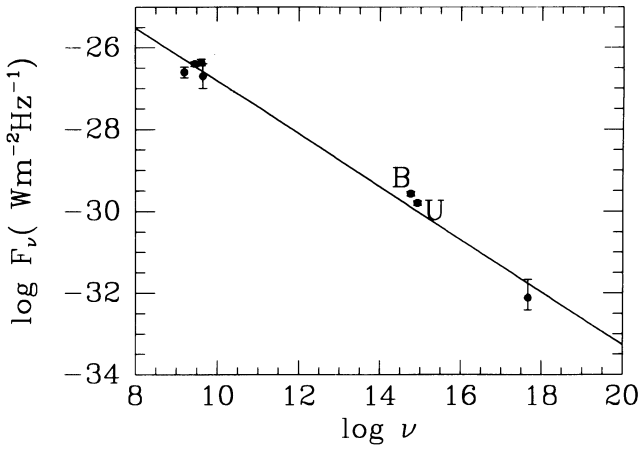

FIG. 5.—Plot of the total flux in various bands. The solid line shows a power law with index 0.58. The X-ray and radio data were obtained at much lower spatial resolution than the *HST* data. *U* and *B* indicate the current *HST* data which are sums of the fluxes from the nucleus and the jet.

3. RESULTS AND DISCUSSION

The jet in NGC 3862 is morphologically similar to the jets seen in M87 and 3C 66B. Indeed, the bifurcation seen at the end of the jet is reminiscent of the "double-stranded" feature seen in the *HST* image of 3C 66B (Macchetto et al. 1991b). The bright knots and the bending seen along the jet can be compared with similar structure seen in and around "knot A" in M87 (Boksenberg et al. 1992).

A careful comparison of Figure 4 and the images in Figure 2 shows that some of the knots may be more strongly emitting in the *B* image. Also, at the point of bifurcation the strands seem to have a higher contrast in the *B* image, although the signal-to-noise ratio is quite low. Thus this jet may have more varia-

TABLE 1

COMPARISON OF JET PARAMETERS

Source	Distance[a] (Mpc)	Size (pc)	α_{opt}	α_{ro}	$\mathcal{F}_\nu$(2 cm) (Jy)	$\mathcal{F}_\nu(B)$ (μJy)
3C 264	86.2	270	1.4	0.58	0.2[b]	93
M87	18	2100	1.2[c]	0.66[d]	4.2[e]	1960[f]
3C 66B	86	≈3000[g]	1.6[h]	0.80[h]	...	9[h]
PKS 0521−036	200	10900[i]	2.0[i]	0.76[i]	0.4[j]	38[f]
3C 273	632	31600	1.33[k]	0.90[l]	2.414[m]	22.1[k]

[a] For $H_0 = 75\ km\ s^{-1}\ Mpc^{-1}$.
[b] Gavazzi, Perola, & Jaffee 1981.
[c] Zeilenger, Moller, & Stiavelli 1993.
[d] Biretta, Stern, & Harris 1991.
[e] Derived from Biretta et al. 1991, Table 5.
[f] Keel 1988.
[g] Macchetto et al. 1991b.
[h] Fraix-Burnet et al. 1989.
[i] Keel 1986.
[j] Flux at 6 cm from Keel 1986.
[k] Röser & Meisenheimer 1991.
[l] Fraix-Burnet & Nieto 1988.
[m] Biretta, Owen, & Cornwell 1989.

tion in spectral index than is seen in the M87 jet. Further observations will have to confirm this.

The absolute fluxes for the nucleus and for the entire jet were determined from the deconvolved images. The nuclear fluxes are $F(342) = 100$ μJy and $F(502) = 174$ μJy. For the jet, the fluxes are $F(342) = 59$ μJy and $F(502) = 93$ μJy. The relative uncertainty in these numbers is estimated to be about 10%, whereas the zero-point error could be bigger by an at present unknown amount. A comparison of fluxes, sizes, and spectral indices for the known optical jets is found in Table 1. This comparison shows that the jet in 3C 264 has approximately the same power in the *B* band, within a factor of 2, as M87 and PKS 0521−036, and 10 times the power of the jet in 3C 66B. This comparison adds strength to the claim that this is the fifth known synchrotron jet. We note, in addition, that the radio-optical spectral index, α_{ro}, for 3C 264 and M87 are similar, with 3C 264 being the softest found so far.

Figure 5 shows the radio, optical, and X-ray fluxes for the nuclear region including the jet. The radio data are taken from the references in Elvis et al. (1981), and from Gavazzi et al. (1981). The X-ray point is from Elvis et al. (1981). Remarkably, the data fall very close to a line with logarithmic slope of 0.58. A definitive interpretation of the data in Figure 5 is not yet possible, since we do not know which part of the radio and X-ray emission comes from the jet and which part comes from the nucleus. We note that the spectral index ($\alpha = 1.4$) found here from the optical data may be due to a cutoff in the synchrotron emission from the jet, as is seen in several other jets (Meisenheimer 1991). Then either the X-ray emission would be associated not with the jet but with the nucleus, or the X-ray emission arises from another process such as inverse Compton scattering.

On the other hand, while most optically detected jets and hot spots show a break in their spectra in the infrared with a spectral index which steepens from about 0.6 to 1.5, two exceptions are known: the 3C 273 jet (Harris & Stern 1987) and the Pictor A hot spot (Röser & Meisenheimer 1987). So, if the X-ray emission is indeed associated with the jet, this would not be so peculiar, but then the spectral index in the optical region would be difficult to reconcile with the scenario suggested by the straight line in Figure 5.

Comparing the morphology, spectral index, total flux, and size with the other known optical synchrotron jets leads us to conclude that there is a high probability that the jet in NGC 3862 is the fifth example of a powerful optical synchrotron jet in an external galaxy. Unfortunately, a more detailed comparison with the other jets is difficult because of the relatively low resolution of the radio data and the need for further optical observations of the spectrum and polarization.

The details of the optical synchrotron emission seen in jets and radio lobes (Crane & Stiavelli 1992) serve as a strong constraint on models for energy transport and for emission mechanisms. Since modeling these sources is an active area of research, and since so few jets are found to have optical emission, further in-depth studies of those sources with optical jets may eventually provide the clue for a definitive model of this fascinating phenomenon.

Finally, we note that 3C 264 has been described as a "boring" elliptical galaxy (Elvis et al. 1981). However, it is a rather typical radio-loud elliptical galaxy with a flat radio spectrum (Gavazzi et al. 1981). Hence it may turn out that *HST* will reveal many new details of the nuclear activity in this kind of galaxy.

It is a pleasure to acknowledge useful contributions to this *Letter* from Bob Fosbury and Klaus Meisenheimer. P. Crane acknowledges support from NASA.

REFERENCES

Baum, S. A., Heckman, T. M., & van Breugel, W. 1992, ApJ, 389, 208
Biretta, J. A., Owen, F. N., & Cornwell, T. J. 1989, ApJ, 342, 128
Biretta, J. A., Stern, C. P., & Harris, D. E. 1991, AJ, 101, 1632
Boksenberg, A., et al. 1992, A&A, 261, 382
Crane, P., & Stiavelli, M. 1992, MNRAS, 257, 17P
Crane, P., et al. 1993, AJ, submitted
Elvis, M., Schreier, E. J., Tonry, J., Davis, M., & Huchra, J. P. 1981, ApJ, 246, 20
Fanaroff, B. L., & Riley, J. M. 1974, MNRAS, 167, 31P
Fraix-Burnet, D., & Nieto, J. L. 1988, A&A, 198, 87
Fraix-Burnet, D., Nieto, J. L., Lelievre, G., Macchetto, F. D., Perryman, M. A. C., & di Serego Alighieri, S. 1989, ApJ, 336, 121
Gavazzi, G., Perola, G. C., & Jaffe, W. 1981, A&A, 103, 35
Harris, D. E., & Stern, C. P. 1987, ApJ, 313, 136
Keel, W. C. 1986, ApJ, 302, 296
———. 1988, ApJ, 329, 532.
Kornneef, J., Bohlin, R., Buser, R., Horne, K., & Turnshek, D. 1985, in Highlights Astron., Vol. 7, ed. J. P. Swings (Dordrecht: Reidel), 833
Lucy, L. B. 1974, AJ, 79, 745
Macchetto, F. D., et al. 1991a, ApJ, 369, L55
Macchetto, F. D., et al. 1991b, ApJ, 373, L55
Meisenheimer, K., Röser, H. J., Hiltner, P. R., Yates, M. G., Longair, M. S., Chini, R., & Perley, R. A. 1989, A&A, 219, 63
Meisenheimer, K. 1991, in IAU Symp. 140, Interstellar and Intergalactic Magnetic Fields, ed. R. Beck & R. Wielebinski (Dordrecht: Reidel)
Paresce, F. 1992, Faint Object Camera Handbook, Space Telescope Science Institute, Version 3.0
Röser, H. J., & Meisenheimer, K. 1987, ApJ, 314, 70
———. 1991, A&A, 252, 458
Sandage, A. R. 1973, ApJ, 183, 711
Véron-Cetty, M. P. 1984, A&AS, 58, 665
Zeilinger, W., Moller, P., & Stiavelli, M. 1993, MNRAS, in press